Experimental Study on G-Band Oversized Backward Wave Oscillator Driven by Weakly Relativistic Electron Beam*)

Shota MAGORI, Kazuo OGURA, Takayuki IWASAKI, Junpei KOJIMA, Kiyoyuki YAMBE, Shin KUBO[1)], Takashi SHIMOZUMA[1)], Sakuji KOBAYASHI[1)] and Kohji OKADA[1)]

Graduate School of Science and Technology, Niigata University, Niigata 950-2181, Japan
[1)]*National Institute for Fusion Science, 322-6 Oroshi-cho, Toki 509-5292, Japan*

(Received 6 December 2013 / Accepted 3 February 2014)

We studied a G-band oversized backward wave oscillator (BWO) driven by a weakly relativistic electron beam of less than 100 kV. Rectangular corrugations are used as slow-wave structures having surface waves with upper cutoff frequencies above 150 GHz (G-band). We examine how dispersion characteristics of surface waves are affected by accuracy in machining the corrugation amplitude, width, and period length. Of these, accuracy in the amplitude has the largest effect. Uniformly distributed annular electron beams are generated by a disk-type cold cathode and injected into the G-band BWO. G-band BWO operations in 137 - 173 GHz and above 173 GHz are achieved by changing the corrugation amplitude. The radiation patterns are fairly broad, and the estimated radiation power is at kW level.

Keywords: oversized backward wave oscillator, weakly relativistic electron beam, cold cathode, slow-wave structure, rectangular corrugation, G-band

DOI: 10.1585/pfr.9.3406032

1. Introduction

High-power microwaves are required for widespread applications such as plasma heating, plasma diagnostics, and radar systems. Slow-wave devices such as backward wave oscillators (BWOs) have been extensively studied as candidates for high- and moderate-power microwave sources. In these devices, a slow-wave structure (SWS) is used to generate slow waves by reducing the phase velocity of electromagnetic waves to the beam velocity. An extremely high output of 3 GW has been achieved by a relativistic X-band BWO [1]. However, high-power operation of a BWO beyond 10 GHz remains difficult. For high-frequency operations, oversized SWSs, whose diameters are much larger than the free-space wavelength of the electromagnetic waves, are suitable. The relativistic diffraction generator and the multi–wave Cherenkov generator are special versions of oversized BWOs, and have produced peak powers above GW levels in the frequency range of up to approximately 46 GHz (Q-band) [2,3]. Such tremendously high-power devices use relativistic MV level pulsed power systems and tesla-level magnetic field systems. For practical applications, operations at reduced voltages and reduced magnetic fields are preferable. In Ref. 4, a power level of approximately 500 MW was achieved at 8.3 GHz (X-band) with a moderate voltage of approximately 500 kV; however, this system still requires a bulky pulsed power system. For lower voltage operations, say 100 kV, the phase velocity of the electromagnetic wave in the SWS should be $0.55c$. Design of oversized SWSs transmitting electromagnetic waves with such a slow phase velocity is difficult because high-frequency operations and lower voltage operations of BWOs are incompatible.

An alternative to BWO for the electromagnetic wave source is the Smith–Purcell free electron laser (SP–FEL). Recently, SP–FEL using the beam of a scanning electron microscope with approximately 30 - 35 kV of voltage and current up to mA order has been demonstrated, and it attracts attention for developing a compact THz source [5,6]. In this SP–FEL, the electron beam passes near the grating surface of an SWS. The electron beam is bunched via interactions with the surface wave of the grating. The bunched electron beam then radiates super–radiant SP emissions. The interaction may result in backward wave or traveling wave operation depending on the group velocity of the surface wave. Super–radiance has not always been observed. Requirements for strong SP radiation based on the backward oscillation have been examined [7]. The electron beam should cover the entire surface of the flat grating. However, in realistic SP–FELs, pencil-like beams partially covered the grating surface, and power levels in the μW range on the grating were reported [5].

By using uniformly distributed annular electron beams, oversized BWOs operating at less than 100 kV have been studied in the K- and Q-bands [8–10]. An annular beam of the order of 100 A completely covers the corrugated surface. Recently, performance of the weakly rela-

author's e-mail: teogura@eng.nigata-u.ac.jp
*) This article is based on the presentation at the 23rd International Toki Conference (ITC23).

tivistic oversized BWO has been improved, and radiation of up to 500 kW (K-band) and 200 kW (Q-band) has been achieved [9]. The quality factor Pf^2 was approximately 3.5×10^5 [kW·GHz^2]. Unique features of these oversized BWOs are (1) use of a cold cathode to obtain a uniformly distributed annular electron beam [11,12], (2) operation by a weakly relativistic electron beam with less than 100 kV, and (3) a guiding magnetic field of less than 1.0 T.

Here, we study a G-band oversized BWO driven by a weakly relativistic electron beam. Our oversized BWO uses SWSs forming surface waves with upper cutoff frequencies from approximately 150 GHz to above 200 GHz (G-band). Electromagnetic waves in this frequency range play an important role in nuclear fusion science. Because making a precise profile such as a sine or other complex curves in the axial direction on the waveguide wall becomes very difficult in the G-band, rectangular corrugations are used. We measure sizes of fabricated corrugation and examine the effects of machining accuracy on SWS's dispersion characteristics. The fabricated G-band SWS is driven by an annular electron beam generated by a disk cold cathode, and G-band BWO operations are studied.

2. G-band SWS

Dispersion characteristics of an SWS are determined by the corrugation amplitude h, corrugation width d, and periodic length z_0. The G-band parameters for the rectangular corrugations used in this paper are listed in Table 1. By decreasing h, the upper cutoff frequency increases. We designed an A-type corrugation with h = 0.15 mm and a B-type corrugation with h = 0.075 mm, which is half of that for the A-type. An amplitude less than 0.01 mm is required; however, fabrication of such corrugations becomes very difficult.

Two configurations for the oversized SWS are considered. One is the rectangularly corrugated waveguide shown in Fig. 1, which has commonly been used in oversized BWOs [2–4, 8–10]. The other is the rectangularly corrugated cylinder shown in Fig. 2, which is an inner corrugation of a coaxial SWS [13, 14]. The rectangularly corrugated cylinder has a cylindrical surface wave (CSW), and has been used in cylindrical SP–FELs based on CSW [15, 16]. Both oversized SWSs are prepared and tested in this study.

Fabricated corrugations are measured using a digital microscope. An example of cross-sectional micrographs is shown in Fig. 3. Measured values of the parameters are listed in Table 1, where A-type is the corrugated waveguide of Fig. 1 with an average radius of 15 mm and B-type is the corrugated cylinder of Fig. 2 with an average radius of 12.5 mm. For both types, machining errors are larger than 0.01 mm for h but less than approximately 0.010 mm for d and z_0.

Dispersion curves with the parameters in Table 1 are shown in Figs. 4 (A-type) and 5 (B-type). In Fig. 4, the surface wave is the TM_{01} mode. The difference in h is approximately 17%, and the upper cutoff frequency changes from 170 GHz to 150 GHz, which is a change of approximately 11%. In Fig. 5, the surface wave is CSW. The difference in h between designed and fabricated corrugations is 0.014 mm (19%), and leads to a 20-GHz (9%) change in operation frequency. A change of approximately 20% in h leads to a change of approximately 10% in the upper cutoff frequency of surface waves. For d and z_0, the measured values coincide with the designed values within 10%, and their effects are smaller than those of h.

Table 1 Comparison of designed and fabricated corrugation parameters.

		h [mm]	d [mm]	z_0 [mm]
A-type	Design	0.15	0.3	0.5
	Fabrication	0.175	0.288	0.503
B-type	Design	0.075	0.3	0.5
	Fabrication	0.061	0.294	0.49

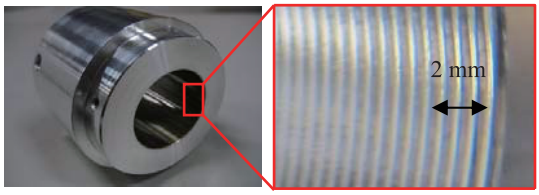

Fig. 1 (left) A-type rectangularly corrugated waveguide. (right) Enlarged photo of the rectangular corrugation.

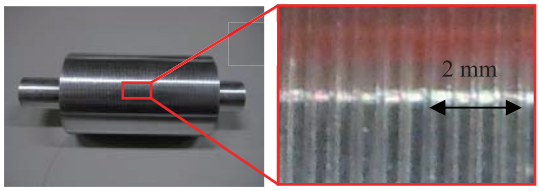

Fig. 2 (left) B-type rectangularly corrugated cylinder. (right) Enlarged photo of the rectangular corrugation.

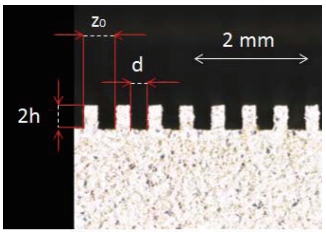

Fig. 3 Cross-sectional micrograph of periodic rectangular corrugation taken by a digital microscope.

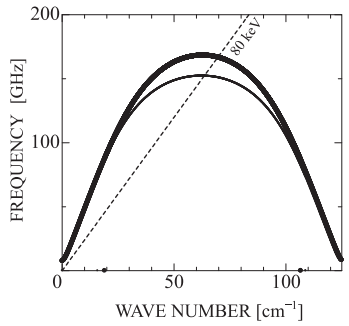

Fig. 4 Dispersion curves of surface wave for A-type slow-wave structure (SWS) of Fig. 1 with parameters listed in Table 1. Thick (thin) solid curves represent designed (fabricated) corrugations. Dotted line is a 80-keV beam line.

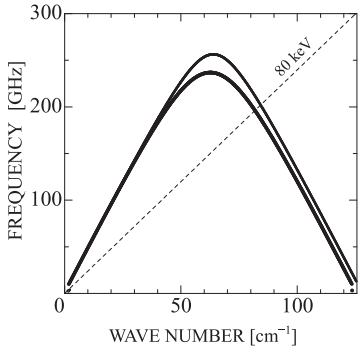

Fig. 5 Dispersion curves of surface wave for B-type slow-wave structure (SWS) of Fig. 2 with parameters listed in Table 1. Thick (thin) solid curves represent designed (fabricated) corrugations. Dotted line is a 80-keV beam line.

3. Experimental Setup

Schematic of the experimental setup is shown in Fig. 6. An output voltage of up to 100 kV from the pulse forming line is applied to a disk-type cold cathode. The disk cathode diameter is 29 mm, and it is made of oxygen-free copper. Uniform annular beams in the weakly relativistic region are obtained with nearly the same diameter as that of the cathode. The thickness of annular beams is typically 2 - 3 mm. For beam propagations, a uniform axial magnetic field B_0 is provided by 10 solenoid coils. In this study, the value of B_0 is 0.8 T. Microwaves are picked up by rectangular horn antennas connected to D-, G-, Y-, and H-band waveguides. The cutoff frequencies are 91, 115, 137, and 173 GHz, respectively.

4. Experimental Results

Typical signals with the A-type corrugation in Fig. 4 are shown in Fig. 7. Time evolutions of the D- and G-band signals were the same. The D-band (G-band) detector had a recommended frequency range 110 - 170 GHz (140 - 220 GHz). These frequency ranges coincided with approximately 150-GHz BWO operation at the crossing point between the TM_{01} and beam line in Fig. 4. Corrugations in Figs. 1 and 2 are formed on the concave side and the convex side of the cylindrically curved surface, respectively. We examined G-band BWOs using two configurations with the same A-type parameters, and found that the configurations in Figs. 1 and 2 have little effect on the radiation. The G-band BWO operation was eventually determined by h, d, and z_0, instead of the SWS configuration.

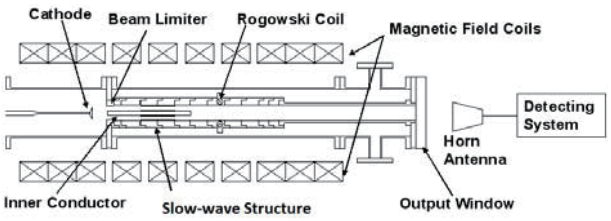

Fig. 6 Schematic of the experimental setup.

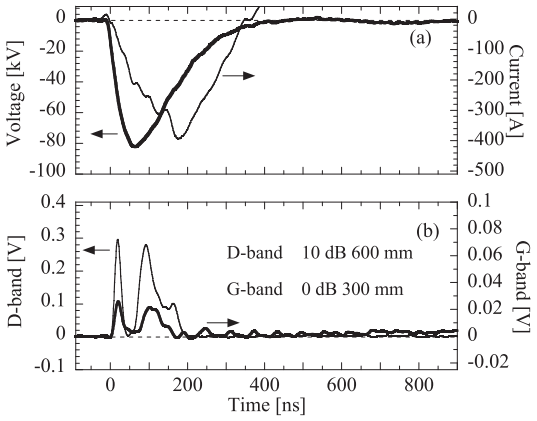

Fig. 7 Waveforms of measured signals: (a) beam voltage and current and (b) D- and G-band signals. Peak value of beam voltage (current) is approximately 80 kV (400 A).

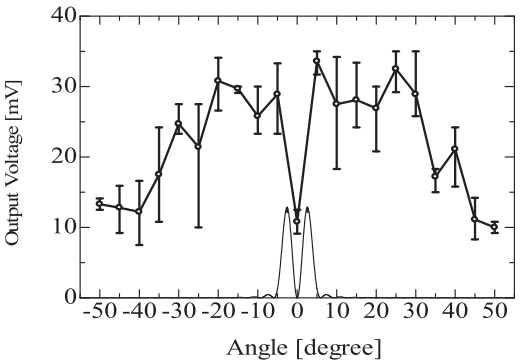

Fig. 8 Radiation pattern with A-type corrugation. G-band system is used and antenna distance from output window is 600 mm. Thin curve is theoretical curve for TM_{01} waveguide mode.

Radiation patterns were obtained by moving a receiving horn antenna in an equatorial plane around a pivot at the center of the output window. Horizontal (E_θ) and vertical (E_φ) components of the electric field were measured. The pattern for E_θ is shown in Fig. 8. As a reference, a

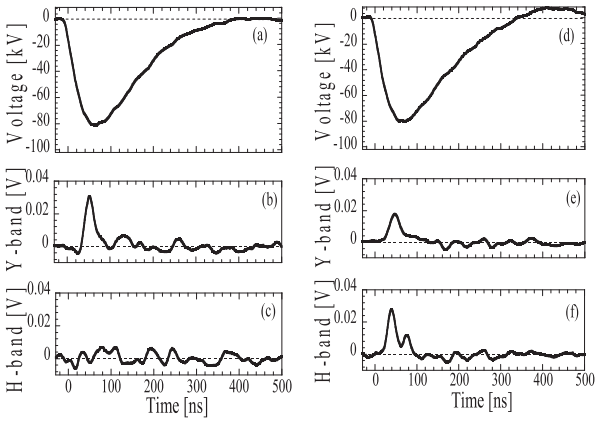

Fig. 9 Waveforms of measured signals for Y- and H-bands. (a) Beam voltage, (b) Y-band, and (c) H-band signals for A-type corrugation. (d) Beam voltage, (e) Y-band, and (f) H-band signals for B-type corrugation.

theoretical radiation curve for the TM_{01} waveguide mode is shown in Fig. 8. It is clear from Fig. 8 that a single TM_{01} mode cannot explain the radiation pattern. Higher order waveguide modes up to approximately TM_{10} are required to explain the radiation spreading beyond 30°. Excited surface waves in the SWS section go into the straight waveguide section before radiating from the output window, as shown in Fig. 6. On the boundary between the SWS and straight waveguide, the excited surface wave couples to the straight waveguide modes, including many higher order modes as well as the lowest TM mode. Pure TM (TE) modes have no E_φ (E_θ) component. In our experiments, both components were detected in the same level; therefore, not only TM modes but also TE modes are included in the coupling on the boundary.

We evaluated radiation power levels. Unfortunately, the G-band detector was not calibrated because of the lack of a proper power source. So, radiation power levels were estimated by the D-band system. The voltages of the D-band detector were calibrated to absolute powers by using a Gunn oscillator at 100 GHz. Considering 10 or 20 dB attenuation in the detecting system, the maximum detected power levels were roughly evaluated to be in W level. By integrating detected power over the broad pattern, the total radiation power in terms of the TM-like mode was estimated to be in kW level.

For the A-type SWS in Fig. 4, microwave signals were detected by the G- and Y-band systems; however the H-band signal was not detected, as shown in Fig. 9. Therefore, the frequency is in the range from the Y-band cutoff (137 GHz) to the H-band cutoff (173 GHz). For the B-type SWS in Fig. 5, the H-band signal appears as shown in Fig. 9. This is consistent with the G-band BWO operation of approximately 200 GHz expected from Fig. 5. Thus, we have demonstrated frequency control of a G-band BWO by changing the corrugation amplitude h of an SWS.

5. Conclusions

A G-band BWO driven by an annular electron beam in a weakly relativistic region of less than 100 kV is experimentally studied. The beam is generated by a disk-type cold cathode. We use rectangular corrugations as the SWS, which have surface waves with upper cutoff frequencies above 150 GHz (G-band). The corrugation sizes of fabricated SWS are measured using a digital microscope, and effects of machining accuracy on the surface waves are examined. Accuracy for h has the greatest effect in our experiment. G-band BWO operations in 137 - 173 GHz and above 173 GHz are performed by changing h. Radiation patterns are fairly broad, and the estimated radiation power is in kW level. G-band BWOs with such intense power in the weakly relativistic region may be of considerable interest for practical use and developing compact THz wave sources.

Acknowledgments

This work was partially supported by Grant-in-Aid for Scientific Research (B) No. 23340173 from the Japan Society for the Promotion of Science and by the NIFS collaboration research program No. NIFS12KLER014.

[1] A.V. Gunin *et al.*, IEEE Trans. Plasma Sci. **26**, 326 (1998).
[2] S.P. Bugaev *et al.*, IEEE Trans. Plasma Sci. **18**, 518 (1990).
[3] S.P. Bugaev *et al.*, IEEE Trans. Plasma Sci. **18**, 525 (1990).
[4] A.N. Vlasov *et al.*, IEEE Trans. Plasma Sci. **28**, 550 (2000).
[5] J. Urata *et al.*, Phys. Rev. Lett. **80**, 516 (1998).
[6] H.L. Andrews *et al.*, Phys. Rev. ST Accel. Beams **12**, 080703 (2009).
[7] V. Kumar and K.-J. Kim, Phys. Rev. ST Accel. Beams **12**, 070703 (2009).
[8] K. Ogura *et al.*, IEEJ Trans. FM **125**, 733 (2005).
[9] S. Aoyama *et al.*, Trans. Fusion Sci. Tech. **51**, 325 (2007).
[10] K. Ogura *et al.*, IEEJ Trans. FM **127**, 681 (2007).
[11] H. Oe *et al.*, J. Plasma Fusion Res. SERIES **8**, 1477 (2009).
[12] K. Yambe *et al.*, IEEE Trans. Plasma Sci. **41**, 2781 (2013).
[13] X. Zheng *et al.*, J. Phys. Soc. Jpn. **64**, 1402 (1995).
[14] K. Ogura *et al.*, IEEE Trans. Plasma Sci. **41**, 2729 (2013).
[15] K. Ogura *et al.*, J. Plasma Fusion Res. **6**, 2401039 (2011).
[16] S. Hasegawa *et al.*, Trans. Fusion Sci. Tech. **63**, 259 (2013).